Miner Deposita (2009) 44:751–764
DOI 10.1007/s00126-009-0245-3

ARTICLE

The geology and mineralisation at the Golden Pride gold deposit, Nzega Greenstone Belt, Tanzania

I. M. A. Vos · F. P. Bierlein · J. S. Standing · G. Davidson

Received: 23 October 2008 / Accepted: 12 May 2009 / Published online: 6 June 2009

Abstract The Golden Pride gold deposit (~3 Moz) is located in the central part of the Nzega Greenstone Belt at the southern margin of the Lake Victoria Goldfields in Tanzania. It represents an inferred Late Archaean, orogenic gold deposit and is hosted in intensely deformed metasedimentary rocks in the hanging wall of the approximately E–W striking Golden Pride Shear Zone. The hanging-wall sequence also includes felsic (quartz porphyritic) to mafic (lamprophyric) intrusions, as well as banded iron formations. Hydrothermal alteration phases associated with mineralisation are dominated by sericite and chlorite. Two main ore types can be distinguished, chlorite and silica ore, both occupying dilational sites and structural intersections in the hanging wall of the main shear zone. Sulphide minerals in both ore types include pyrrhotite, arsenopyrite, pyrite and accessory sphalerite, galena, sulphosalts and Ni–Co–Bi sulphides. Gold and tellurides are late in the paragenetic sequence and associated with a secondary phase of pyrrhotite deposition. Sulphur isotope compositions range from −6 to 7 per mil and are interpreted to reflect contributions from two distinct sources to the mineralising fluids in the Golden Pride gold deposit. A redox change, potentially induced by the intrusion of mafic melts, together with structural elements in the hanging wall of the Golden Pride Shear Zone, are interpreted to be the main controls on gold mineralisation in this deposit.

Keywords Lake Victoria Goldfields · Tanzania
Orogenic gold · Golden Pride · Late Archaean

Editorial handling: B. Lehmann

Electronic supplementary material The online version of this article (doi:10.1007/s00126-009-0245-3) contains supplementary material, which is available to authorized users.

I. M. A. Vos
Resolute Tanzania Limited,
P.O. Box 78486, Plot 1670, Mwaya Road, Masaki,
Dar es Salaam, Tanzania

I. M. A. Vos · F. P. Bierlein
School of Earth and Environment,
University of Western Australia,
Crawley, Western Australia 6009, Australia

J. S. Standing
Jigsaw Geoscience Pty. Ltd.,
P.O. Box 488, West Perth, Western Australia 6872, Australia

G. Davidson
ARC Centre of Excellence in Ore Deposits,
University of Tasmania,
Private Bag 79,
Hobart, Tasmania 7001, Australia

Present Address:
I. M. A. Vos (✉)
SRK Consulting,
Suite 2100, 25 Adelaide Street East,
Toronto, Ontario M5C 3A1, Canada
e-mail: ivovos@srk.com

Present Address:
F. P. Bierlein
Afmeco Mining and Exploration Pty. Ltd.,
80 Leader Street,
Forestville, South Australia 5035, Australia

Introduction

The Late Archaean Lake Victoria Goldfields (LVG) in Tanzania represent a comparatively underexplored and poorly understood, highly endowed amalgamation of terranes, which hosts several world-class gold deposits, including operating mines at Geita, Bulyanhulu, Buzwagi and North Mara (Fig. 1). The LVG shows many similarities with other highly endowed Late Archaean greenstone terranes, such as the Yilgarn Craton in Western Australia and the Abitibi Province in Canada (Hagemann and Cassidy 2000).

A better understanding of the genesis of and structural controls on gold mineralisation, such as fluid sources and relationships between ore formation and magmatism in the LVG, will aid conceptual targeting strategies that have proven highly successful in more mature terrains such as the Eastern Goldfields Province of the Yilgarn Craton in Western Australia (e.g. Groves et al. 2003). In addition, deposit-scale studies, like our current study, may contribute to multi-disciplinary and scale-integrated studies that could address the current dearth of knowledge on the tectono-metallogenic evolution of the LVG.

This paper provides a comprehensive study of the geology and ore paragenesis of the Au Golden Pride gold deposit following an earlier study by Stevens and Kennedy (1998, i.e. prior to mine development). The Golden Pride Mine (~60 Mt at 1.6 g/t in reserves and measured + indicated resource) is an open pit carbon-in-leach mine with an annual production of 2.5 Mt at an average head grade of 2 g/t from sulphide and oxidised ore. We describe the local stratigraphy and mineralisation styles based on lithological, structural, petrographical and geochemical investigations of diamond drill core supplemented by observations from the open pit mine. Supporting ore paragenesis and sulphur isotope studies have been carried out to further constrain the nature and source of the mineralising fluids at the Golden Pride gold deposit.

Regional geological setting

The LVG comprise a number of E–W to NW–SE striking super-terranes that can be subdivided into terranes and belts (Kabete et al. 2008). The greenstone belts in the LVG are comprised of dominantly mafic volcanic rocks and (immature) sedimentary rocks that are assigned to the Late Archean Nyanzian Supergroup (Borg 1990; Borg and Shackleton 1997). The super group can roughly be divided into a Lower and Upper Series on the basis of a recognisable upward transition from mafic to felsic lavas, with minor tuffs and interbedded sedimentary rocks. Recently, a LVG-wide geochronology study supported by

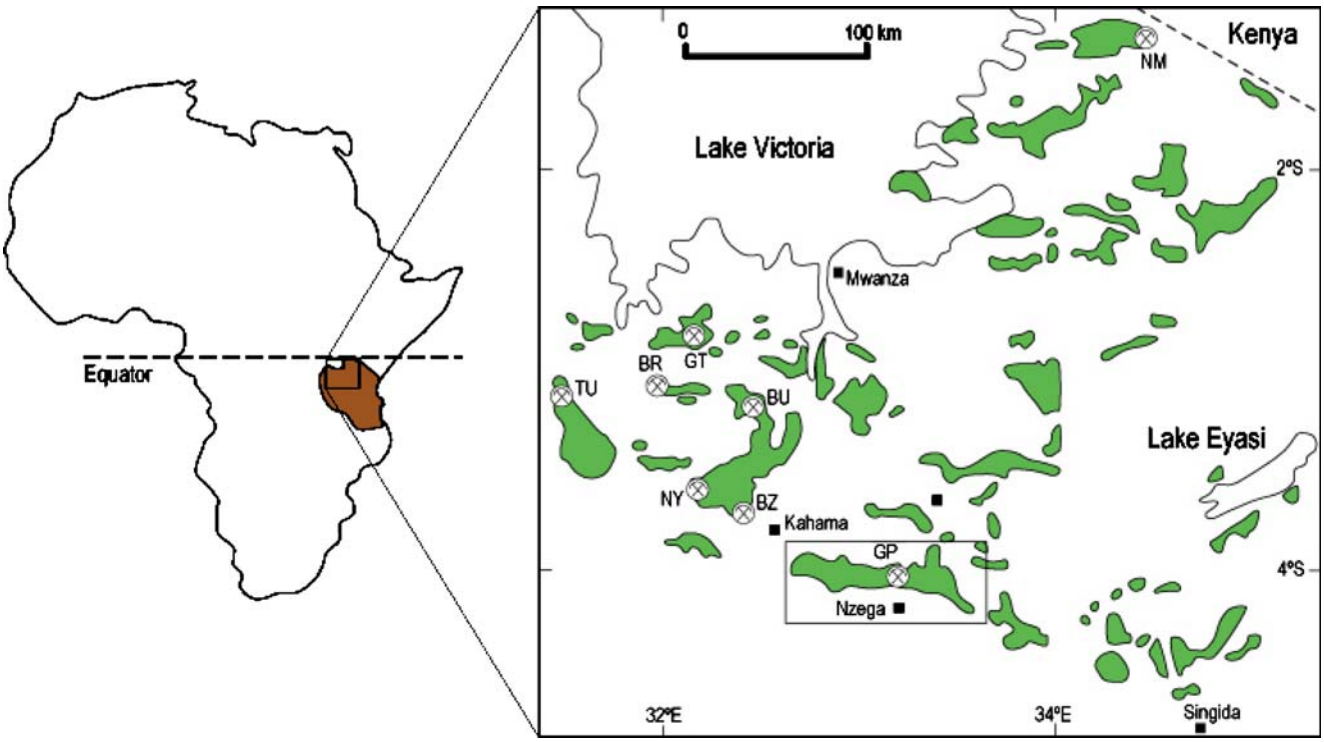

Fig. 1 Overview map of greenstone belts (*in green*) and major gold deposits in the Lake Victoria Goldfields, northern Tanzania. *Inset* refers to extent of Fig. 2. Gold deposits indicated on map include: Tulawaka (*TU*), Geita (*GT*), Bulyanhulu (*BU*), Buck Reef (*BR*), Nyakafuru (*NY*), Buzwagi (*BZ*), Golden Pride (*GP*) and North Mara (*NM*). Image adapted after Borg and Shackleton (1997)

several mining and exploration companies operating in Tanzania has been conducted (Chamberlain and Tosdal 2007). This study has indicated that the geological history of the greenstone belts in Tanzania is more complex than previously suggested. It is suggested that the Nyanzian Supergroup is made up of supra-crustal sequences that evolved in different isolated basins or arcs at different times that subsequently amalgamated during collision. A better defined subdivision of the Nyanzian Supergroup stratigraphy may better represent these characteristics. The reader is referred to the work of Kabete et al. (2008) that addresses some of the issues related to the geological evolution of the LVG.

The Golden Pride gold deposit is situated in the Nzega Greenstone Belt (NGB) of the Nzega–Sekenke Terrane (Fig. 2; Kabete et al. 2008). The Nzega–Sekenke Terrane forms the southernmost portion of the LVG and is juxtaposed against the Dodoman Granite-Gneiss Belt to the south (Harpum 1970). To date, very little work has been carried out to understand the geological history of the NGB. A general description of stratigraphy and structures is provided in this paper.

The NGB is an E–W trending greenstone belt that contains volcanic and sedimentary rocks belonging to both the Upper and Lower Nyanzian Series (Borg 1990; Borg and Shackleton 1997). The belt is thick at its western and eastern ends and narrow in the centre. As indicated on Fig. 2, a number of gold camps have been recognised within the NGB, which include the Golden Pride gold deposit. In addition, several diamondiferous kimberlite pipes (or plugs) occur within the belt. Thick sequences of mafic meta-volcanic rocks occur at both ends of the belt. In the east of the belt, rhyolitic to dacitic meta-volcanic and meta-volcano-sedimentary rocks occur with the mafic rocks. Borg and Krogh (1999) obtained a U–Pb age date of 2,780±3 Ma from rhyolite pyroclastics in the adjoining greenstone belt that could potentially be associated with the rhyolitic volcanic rocks in the eastern end of the NGB. The rest of the belt is characterised by greenschist facies, fine-to medium-grained siliciclastic rocks interbedded with banded iron formations (BIFs). At the Golden Pride mine, a U–Pb age date of 2,716±11 Ma was obtained from a homogenous zircon population derived from meta-sandstone interbedded with BIF (Chamberlain and Tosdal 2007). The Nyanzian rocks are unconformably overlain by polymictic conglomerates and sandstones associated with the Kavirondian System. In the NGB, the presence of these sedimentary rocks is commonly associated with large shear systems and U–Pb dating of zircon populations derived from these rocks indicated major contributions from source rocks with ages of 2,650 to 2,680 Ma (Chamberlain and Tosdal 2007), suggesting that the Kavirondian System

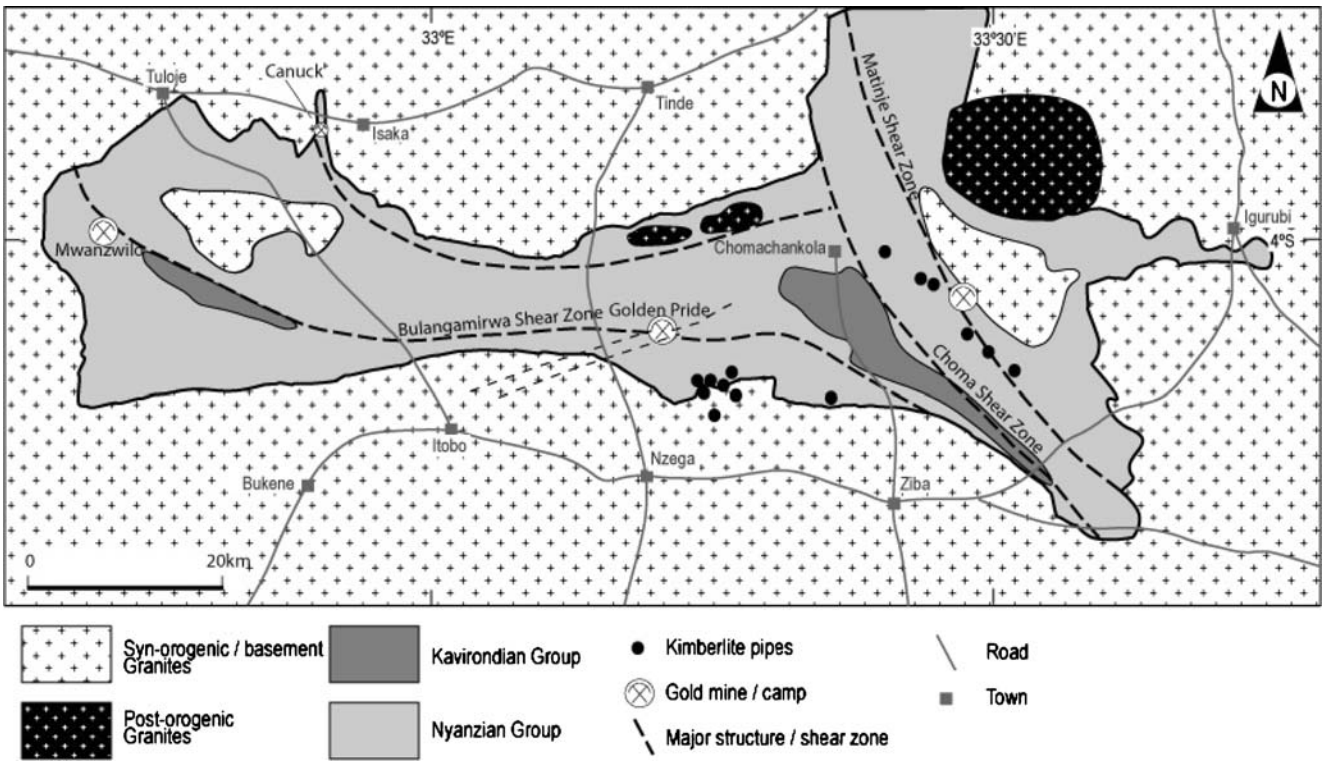

Fig. 2 Regional geological map of the Nzega Greenstone Belt indicating main stratigraphic division, structures and gold mines/camps. The Golden Pride gold deposit is located just east of the centre of the belt

developed <2,650 Ma. The most prominent shear system in the NGB is the ~150 km long, generally E–W trending Bulangamirwa Shear Zone situated centrally in the NGB. Due to its vicinity to the Golden Pride gold deposit in the central part of the NGB, the local name adapted for this shear zone is the Golden Pride Shear Zone (GPSZ).

In areas away from shear zones, the dominant structural style is macro-scale folding. Two stages of folding are preserved: (1) early, belt-parallel isoclinal folds (F_1) with rarely observed axial planar foliation (S_1) and (2) late, upright, open to close folds (F_2) with well-developed axial planar foliation (S_2) representing the dominant foliation. Within or close to the major shear zones, S_2 is overprinted by a strong shear foliation. The Kavirondian System rocks are folded by F_2, but not affected by F_1, indicating that deposition of these rocks post-dated the earliest recorded phase of compression (F_1).

The metamorphic grade within the NGB is dominantly greenschist facies, and all lithotypes described within this paper have been subjected to lower greenschist facies metamorphism. More intense metamorphism can be observed along the southern margin of the belt, where mafic volcanic rocks are metamorphosed to amphibolite facies and sedimentary rocks display large porphyroblasts of andalusite.

Analytical methods

Drill core study and open pit mapping

Extensive lithological and structural re-logging of representative drill holes sampling fresh rock at depth was carried out in 2006 to determine the mine stratigraphy and develop a 3D geological model. In addition, pit mapping of accessible exposures was carried out to investigate structural elements that could be recognised in the fresh rocks exposed in the walls of the open pit. As part of this study, representative samples from each observed lithotype were selected for petrographical and geochemical work.

A selection of 37 meta-sedimentary and mineralised rock samples was investigated using standard optical petrographic and mineragraphic methods. This included the optical inspection of fluid inclusions in mineralised quartz vein samples at high magnifications. In addition, a selection of 21 igneous rock samples was analysed by standard optical petrographic methods only.

Furthermore, a selection of 25 samples, representing each lithotype and style of mineralisation at the Golden Pride gold deposit, was sent to ALS Laboratory in Perth, Australia, for whole-rock and multi-element analysis. These methods comprise whole-rock analysis by X-ray fluorescence (XRF) and multi-element analysis after four-acid digestion by combined inductively coupled plasma mass spectroscopy (ICP-MS) and inductively coupled plasma-atomic emission spectrometry, respectively. Low-detection limit gold assays were carried out for each sample from aqua regia digestion with atomic absorption spectroscopy finish.

Ore paragenesis study

A selection of 44 polished thin sections were studied by ore microscopy at the University of Australia, and additional scanning electron microscope (SEM) work on these sections was carried out at the University of Ballarat using a JeolTM JSM 6300 SEM. Backscattered wavelength-dispersive electron (BSE) images and energy dispersive X-ray spectroscopy (EDS) data were acquired using an Oxford Instruments four element quadrant detector. The applied electron beam conditions were 15 kV and 1.5 nA for BSE imagery and between 20 and 30 kV and 5 nA for quantitative EDS analysis.

Sulphur isotope study

A total of 13 individual monomineralic sulphide samples were extracted from 12 specimens using a micro-drill, followed by magnetic and heavy liquid separation methods and checking for impurities. Small amounts of impurities (e.g. sphalerite, chalcopyrite) were retained in some cases due to intimate intergrowth of the three principle sulphide phases in these samples. The separated sulphides (i.e. pyrite, pyrrhotite, arsenopyrite) were converted to SO_2 under vacuum at 900°C using Cu_2O as an oxidant. Sulphur isotope ratios were determined for the purified SO_2 on a mass spectrometer dedicated to sulphur isotope determinations at the Central Science Laboratory of the University of Hobart. Seven samples were deemed suitable for multiple in situ laser ablation analysis of individual sulphide grains. The chief advantage of this technique is that sulphide grains as small as 200 μm in diameter may be analysed for their $\delta^{34}S$ isotope compositions, which is ideally suited for potentially chemically zoned sulphide grains of uncertain genesis in the vicinity of gold deposits. A detailed description of the laser ablation technique for sulphur isotope analyses, as employed at the University of Tasmania, is provided by Huston et al. (1995). The technique requires the preparation of doubly polished 'thick sections', similar to those used for fluid inclusion microthermometric analyses. A total of 16 in situ analyses were undertaken on a Quantronix model 117 Nd:YAG laser.

Stable sulphur isotope ratios ($\delta^{34}S$) are reported relative to the Canyon Diablo Triolite (CDT) in parts per mil (‰). Error margins and precision values for in situ and conventional analyses are typically 0.05‰ and 0.1‰, respectively (Huston et al. 1995).

Geology of the Golden Pride gold deposit

Mine stratigraphy

Detailed lithological and structural inspection of drill core, together with pit mapping, from the Golden Pride gold deposit show that the mine stratigraphy mainly comprises a series of strongly foliated, lower- to middle-greenschist facies, interbedded sandstone and siltstone units. This sequence is intersected by intensely foliated (i.e. schistose) and carbonate-altered rocks that represent the GPSZ, which divides the mine stratigraphy into a hanging wall and a footwall sedimentary sequence. In close spatial association with the GPSZ and related structural elements, a variety of intrusions crosscut the mine stratigraphy. Furthermore, BIF units occur within both the hanging wall and footwall sedimentary sequence. An example of a typical cross section through the Golden Pride gold deposit is presented in Fig. 3.

Hanging-wall sedimentary sequence

The hanging-wall sedimentary sequence is dominated by interbedded meta-sandstones and meta-siltstones of variable grain size (Fig. 4a), in which a general increase in the volume of siltstone relative to sandstone can be observed towards the south. Sandstones range from fine- to coarse-grained gritty units. Within this sequence, primary sedimentary structures and textures such as graded bedding, cross-bedding and rip-up clasts are well preserved. Individual beds vary in thickness from 1 mm (laminated siltstone and shale) to several metres (occasionally >20 m). These rocks have undergone variable degrees of chlorite, biotite and sericite alteration. Rare turbidite/density flows are also observed in the drill core, which together with other sedimentary features may indicate that at least part of the sequence may represent turbidite deposits. Tight to isoclinal folding of bedding is observed, with axial planar cleavage best developed in mica-rich rocks. In rare cases, graded bedding has been observed to be reverse over a 5 m interval highlighting the tightness of folding. This sequence hosts the bulk of gold mineralisation at the Golden Pride gold deposit.

Sparse discrete units of BIF are present within the hanging-wall sedimentary sequence. These BIF units do not carry any gold mineralisation and are generally composed of bands of massive magnetite (oxide facies), or magnetite-bearing meta-sediments, and re-crystallised chert up to several centimetres thick. The units vary from 0.5 to 5 m thick, but are commonly ~1 m wide. They may be traced in the pit for hundreds of metres, but generally occur as strongly folded discontinuous units that are not associated with mineralisation.

Two types of BIF units can be distinguished: (1) interbedded silty to sandy iron-rich (i.e. magnetite-bearing) units of approximately 5 cm thickness interlayered with meso-bands of white-grey chert and minor dark green bands of dolomite–magnetite-altered meta-sediments and (2) magnetite + calcite + chlorite-altered siltstone bands interbedded with chlorite + biotite + magnetite-altered siltstone bands lacking the presence of cherty meso-bands (Fig. 4b). In places, the latter may be altered to pyrrhotite–magnetite bands interlayered with chlorite + garnet + magnetite-rich veins.

Several, structurally displaced, dacitic porphyries intrude the hanging-wall sedimentary sequence. These porphyries vary in quartz and plagioclase phenocryst content and size, up to a mega-crystic plagioclase–biotite porphyry. The porphyries are variably hydrothermally altered, resulting in sericitisation and albitisation. Also, the presence of leucoxene was noted, which may be replacing minor amounts of

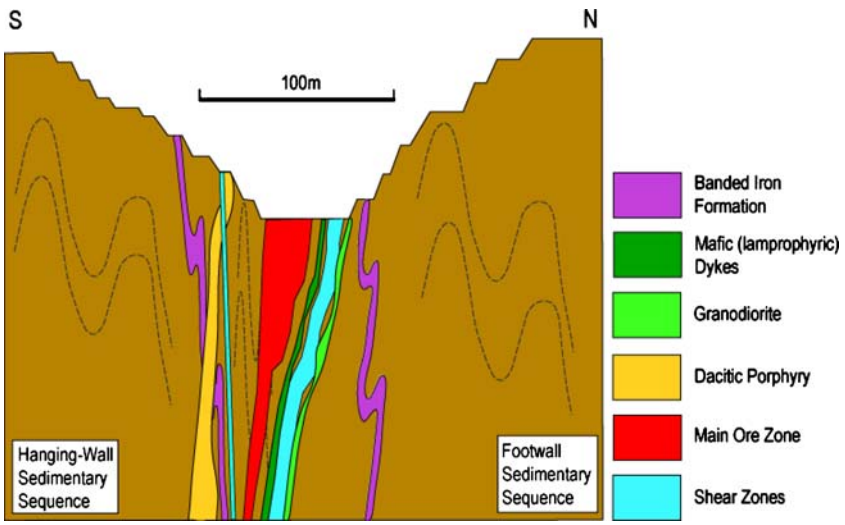

Fig. 3 Schematic cross-section of the mine stratigraphic sequence at the Golden Pride gold deposit

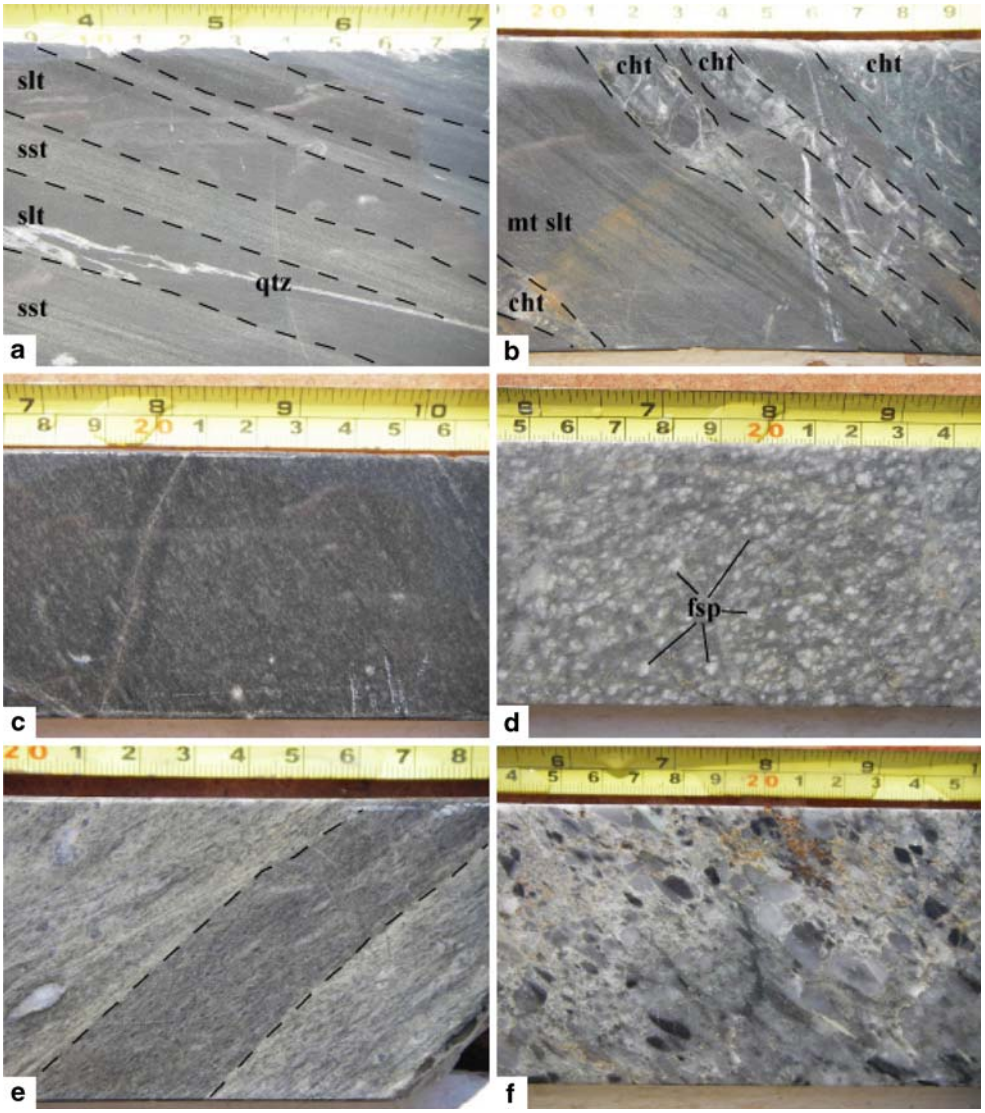

Fig. 4 Representative images of the main rock types found in the Golden Pride Au deposit stratigraphy. **a** Interbedded sandstone (*sst*) and siltstone (*slt*) sequence. Note the folded quartz vein (*qtz*) in the siltstone bed near the bottom of the image. **b** Banded iron formation (type 1) consisting of interbedded magnetite-rich siltstone (*mt slt*) bands and chert (*cht*) mesobands. **c** Equigranular granodiorite. **d** Dacitic porphyry with numerous feldspar (*fsp*) phenocrysts. **e** Lamprophyric dykelet intruding earlier mafic dyke. **f** Polymictic conglomerate consisting mainly of chert pebbles

primary magmatic Ti-rich biotite and/or Fe–Ti oxides. In some cases, spatially restricted albite–hematite alteration can be observed within porphyries. The porphyries are commonly characterised by moderate to high Sr/Y ratios (Table 1, Electronic Supplementary Material), indicative of an origin by deep crustal melting (e.g. Tulloch and Kimbrough 2003). Chamberlain and Tosdal (2007) obtained a U–Pb age of 2,680±15 from a porphyry sample from the Golden Pride mine.

Discontinuous, narrow (tens of centimetres thick), strongly foliated and carbonate-altered, variably amygdaloidal and/or fuchsite-bearing dykes (Fig. 4e) are spatially closely associated with the GPSZ. Whole-rock geochemical analyses from dyke samples indicate unusually high Nb, Ti, P, Ce, Th and Cr values (mafic intrusions in Table 1, Electronic Supplementary Material), and petrographic investigations indicate the presence of abundant plagioclase phenocrysts and former mafic phenocrysts (generally replaced by chlorite, but in places recognised as biotite, olivine and/or apatite). These observations suggest that these mafic intrusions may be of lamprophyric affinity. The intense and relatively coarse-grained carbonate alteration suggests that the original magmas from which these mafic intrusions were generated were carbonate-rich (A.J. Crawford 2007, written communication).

Footwall sedimentary sequence

The footwall sedimentary sequence is similar to the hanging-wall sedimentary sequence in terms of its sandstone–siltstone intercalation and sedimentary features observed within the rocks. However, this sequence contains at least two distinct conglomerate units: a coarse-grained siliceous polymictic conglomerate unit with rounded quartz and chert clasts ranging in size from 2 mm to 2 cm (Fig. 4f) and a monomictic pebble conglomerate containing rounded

chloritoid- and sericite-altered sandstone clasts. Also, a distinctive folded BIF unit (type 1—above) up to 20 m wide is present in the footwall sedimentary sequence.

A granodiorite intrusion represents the only intrusive rock type observed in the footwall sequence. This intrusion occurs directly in the footwall to the GPSZ and consists of aphyric, equigranular and medium-grained (micro-)granodiorite (Fig. 4c) that is strongly sericite–carbonate altered. Elevated Ti, P, Sr, Nb and Cr (Table 1, Electronic Supplementary Material) concentrations suggest that the granodiorite intrusion could be genetically related to the dacitic intrusions observed in the hanging wall and may represent the 'intermediate' magmatic phase between the feldspar(-quartz) porphyries and mafic intrusions (Wilson 1989).

Alteration

Alteration assemblages observed within the meta-sedimentary rocks of the Golden Pride mine stratigraphy can be broadly divided into two groups: (1) proximal alteration assemblages common in strongly deformed domains that host the ore zones in the immediate hanging wall of the GPSZ and (2) distal alteration assemblages that occur mostly in less deformed parts of the mine stratigraphy. Both types of alteration are dominated by the presence of sericite and chlorite with minor biotite, chloritoid and pyrrhotite. A notable difference can be observed in chlorite alteration that is marked by distinctly iron-rich chlorite in close vicinity to the GPSZ, in comparison with magnesium-rich chlorite further away from the GPSZ (Vos et al. 2007).

Deformation and structure

The structural setting of the Golden Pride deposit is dominated by the presence of the GPSZ and large-scale tight to isoclinal folding. Timing relationships within the deposit indicate that the development of the GPSZ and related elements occurred contemporaneous with, and postdates the emplacement of, intrusions and formation of folds. The 5–20 m wide GPSZ forms the dominant structure controlling a series of shears that can be observed in the mine. It strikes approximately 100° and dips steeply to the south. The hanging-wall shear (HWS) is another prominent structure, located approximately 40–50 m to the south of and parallel to the GPSZ. The HWS forms a several metres-wide shear zone characterised by distinctive strong chlorite alteration associated with shear fabrics and weakly mineralised, strongly boudinaged quartz–pyrite–pyrrhotite veins. This structure dips steeply to the north near the surface and cross-cuts the dacitic porphyry and BIF units. Other structures include a set of WNW–ENE trending cross-structures that link up with the GPSZ and late-stage N-dipping thrust faults that offset mineralisation for several metres.

Meso-scale (hundreds of metres) tight to isoclinal upright to inclined folds $\left(F_1^{GP}\right)$ are considered parasitic to regional scale folds in the NGB (F_1). This is consistent with the numerous younging and vergence direction reversals observed in drill core. Fold axes have variable plunges that appear to be dominated by moderate to steep eastward plunge directions. This folding is associated with the development of a semi-penetrative axial planar foliation $\left(S_1^{GP}\right)$ that cuts bedding at low angles.

A steeply dipping penetrative cleavage $\left(S_2^{GP}\right)$ overprints S_1^{GP} within the mine. Bedding and S_1^{GP} are strongly transposed by the S_2^{GP} foliation and generally trend ~110° (Fig. 5). An acute angle between S_1^{GP} and S_2^{GP} may be observed (Fig. 6), but, approaching the HWS from the south, the intensity of deformation and foliation $\left(S_2^{GP}\right)$ increases, whereby S_2^{GP} completely obliterates S_1^{GP} in the vicinity of the GPSZ, and preservation of earlier fabrics is restricted to low strain boudins and lenses sandwiched between D_2^{GP} shears. The bulk of S_2^{GP} fabric formed during oblique sinistral reverse shearing as inferred from kinematic indicators such as s–c fabrics, secondary shear bands, asymmetric pressure shadows and drag folding of veins.

Mineralisation and veining

Distribution and grade

Gold mineralisation occurs in irregular pods distributed along a 3 km length of the GPSZ within the mine area. At depths of 30–40 m within the oxidised profile, mineralisation widths vary from 20 to 95 m using a typical 0.5 g/t grade cutoff. Within the western portion of the main pit, a typical section through the orebody at a depth of 100 m below surface will expose mineralisation over a horizontal width of 65 m at a grade of 2.6 g/t. The poddy distribution is interpreted to be the result of structural control on mineralisation, whereby dilational zones along the intersection of WSW–ENE trending structures and the E–W trending GPSZ and HWS may have been the focus for gold deposition. In addition, modelling of the outlines of the GPSZ with grade control data has indicated that moderately eastward-plunging high-grade ore shoots are parallel to meso-scale warping and bending in the shear zone (Fig. 7), suggesting strong structural control on mineralisation.

Ore characterisation

Two main ore-bearing lithotypes can be recognised within the Golden Pride mine sequence. Differences between the two are most likely controlled by the composition of the

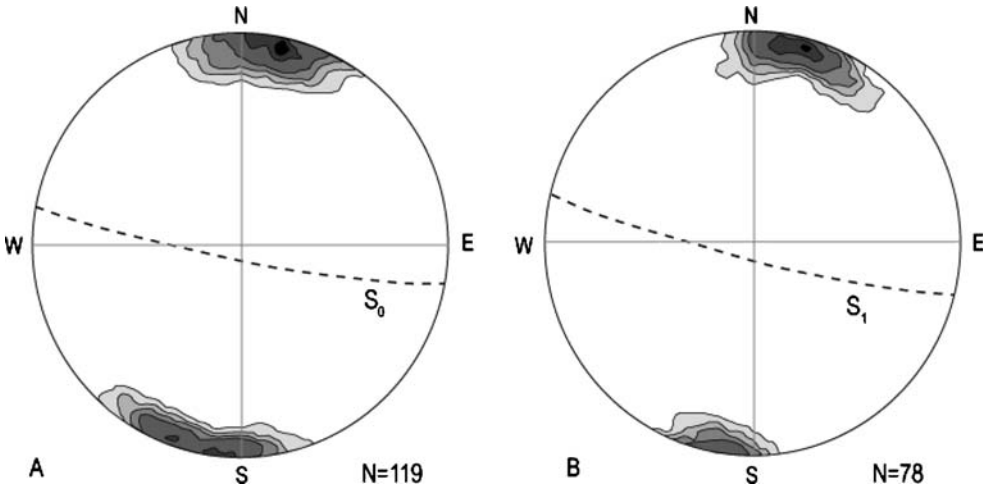

Fig. 5 Equal area, lower hemisphere stereonet projections of bedding (**a**) and foliation (**b**) within the Golden Pride deposit

protolith. Within both types, mineralised veins are developed concordant and discordant to bedding as well as S_2^{GP}, and vein shapes are commonly modified by post-veining deformation. In addition to these ore types, sulphidation of host rocks is evident from the presence of irregular, up to several metres wide areas of disseminated sulphides (mainly pyrite) around the margins of the ore zones. Although a variety of textures and parageneses can be observed between the two end-member styles, the main characteristics of the two ore-bearing lithotypes can be summarised as follows:

1. Chlorite ore

Chlorite ore at the Golden Pride gold deposit is predominantly associated with interbedded siltstones and finer-grained sandstones in the hanging wall of the GPSZ as well as around the HWS. This type of ore is characterised by the presence of pyrrhotite- and pyrite-bearing chlorite–biotite–quartz–calcite shear veins (Fig. 8b, c). Pyrrhotite forms fine-grained wispy masses that overprint foliation and quartz veining. Elevated gold grades (>10 g/t Au) in the chlorite ore are associated with arsenopyrite development along shear fabrics, irregular quartz–chlorite shear veins and higher overall sulphide content. Visible gold and rare chalcopyrite can be observed within the chlorite ore.

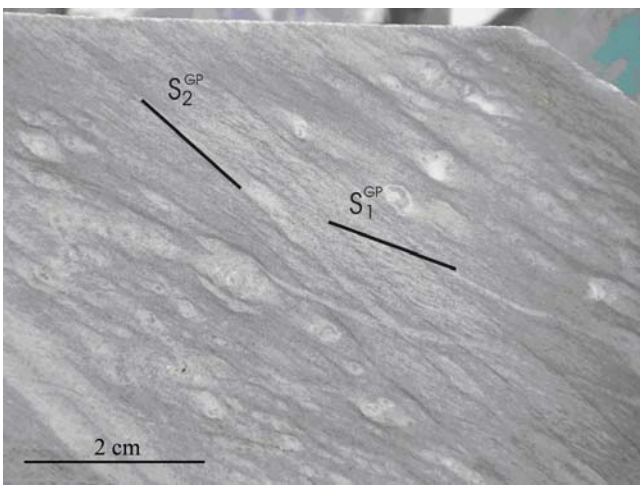

Fig. 6 Example of S_1^{GP} and S_2^{GP} development in a foliated mafic intrusive occurring in low-strain boudin close to the GPSZ

2. Silica ore

The silica ore at the Golden Pride gold deposit is characterised by strong silicification of the protolith (Fig. 8a) and is hosted by coarse-grained sandstones and less commonly intrusive rocks in the hanging-wall to the GPSZ. The intensity of silicification can vary between 20% and 80% and is generally manifested by smoky grey, re-crystallised and re-cemented quartz with minor pyrrhotite, arsenopyrite and rare visible gold (commonly in late fractures). The silica ore has a poddy distribution along strike, potentially as a result of the geometries displayed by the fold patterns within the host sandstone and/or controlled by fault intersections. Silica ore displays a variety of textures including (a) breccia quartz veins in which dark re-crystallised quartz contains angular clasts of quartz–sericite–arsenopyrite-altered sedimentary rocks, (b) massive veins, shear veins and breccia quartz veins in zones of intense silicification and (c) late irregular calcite (± pyrrhotite) veins.

Ore paragenesis

A paragenetic sequence, as inferred from textural relationships observed in both thin section and SEM analysis, is shown in Fig. 9. Drill core observation supplemented by petrographic studies indicates that the dominant sulphide minerals at the Golden Pride gold deposit are, in order of abundance, pyrrhotite, arsenopyrite, pyrite and chalcopyrite. Textural relationships indicate that ductile deformation affected a post-peak metamorphic sulphide assemblage.

This assemblage is mainly characterised by an early phase of disseminated pyrrhotite (po_1) which displays annealing, 120° triple junction grain boundaries and twinning (Fig. 10a), together with commonly fractured and rotated pyrrhotite and arsenopyrite (Fig. 10b) that occurs with later sulphides and gangue minerals in pressure shadows in zones of higher strain. Minor magnetite and pyrite are observed in association with this assemblage. Relatively silver-rich (≤17 at.% Ag; Table 2, Electronic Supplementary Material) gold appears to be emplaced more or less synchronous with an assemblage of dominantly vein-associated pyrrhotite + pyrite ± chalcopyrite ± sphalerite ± galena (Fig. 10c) following incipient destruction of early magnetite and arsenopyrite. The second phase of pyrrhotite (po_2) in this assemblage is subtly enriched in iron (47.2 at.% average, versus 46.7 at.% in po_1; Table 2, Electronic Supplementary Material) and depleted in sulphur (52.3 versus 53.2 at.% in po_1; Table 2, Electronic Supplementary Material). Gold occurs as free gold in cracks and inclusions within Fe sulphides (mainly arsenopyrite; Fig. 10d) and, in rare cases, as interstitial inclusions within carbonate–silicate gangue minerals. Another phase of pyrite deposition commenced during or shortly after the main gold phase and continues together with the deposition of sulphosalts, stibnite and Ni–Co–Bi sulphide phases in (micro-) veinlets that also occur with minor gold (Fig. 10e). SEM study further revealed the presence of relatively minor amounts of low-Fe (approximately 6%) sphalerite and galena, gold and trace amounts of gersdorffite (NiAsS), breithauptite (NiCoSb), gudmundite (FeSbS), willyamite (CoNiSbS), tetradymite (Bi_2Te_2S), ullmannite (NiSbS), electrum (AuAg) and a range of other unidentified bismuth tellurides, gold–bismuth–antimony sulphides and silver–bismuth–tellurium antimonides. Magnetite, ilmenite, scheelite and rutile also form accessory phases in some of the mineralised sections studied.

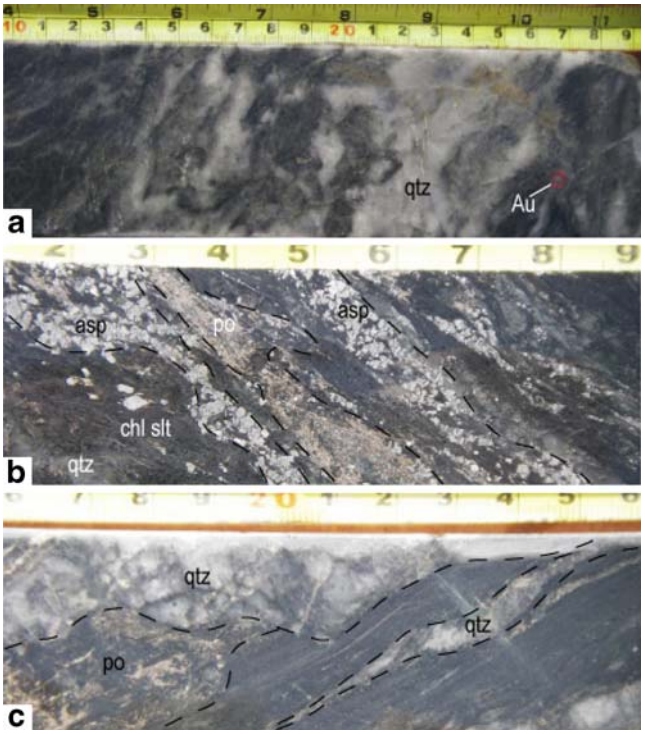

Fig. 8 Images of representative sections of ore for the Golden pride Au deposit. **a** Silica ore showing the strong silicification of sericite-altered sandstone. **b** Chlorite ore showing arsenopyrite- and pyrrhotite-rich bands within chlorite-altered siltstone. **c** Chlorite ore showing a pyrrhotite-rich domain amongst strongly boudinaged and deformed quartz veins within chlorite-altered siltstone

Microscopic inspection of fluid inclusions in vein quartz indicated the presence of at least two generations of liquid + vapour inclusions (Fig. 10f). The most common inclusions have fluid > gas ratios (*FL+V*), whereas a small proportion of inclusions have large bubbles that almost completely fill the negative crystal-shaped inclusions (V rich). The latter

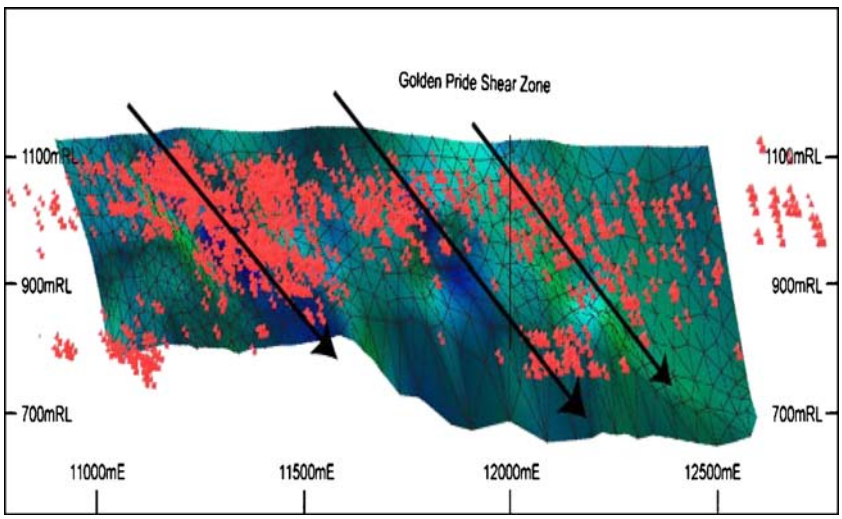

Fig. 7 Long section (local mine coordinates) of east–west trending modelled shear zone envelope for the GPSZ, indicating a number of bends along the envelope (*black arrows*) coinciding with the orientation of high-grade ore shoots as highlighted by *red triangles* (>5 g/t Au assays). Image adapted from original by Mr. I. Neilson (Jigsaw Geoscience Pty. Ltd.)

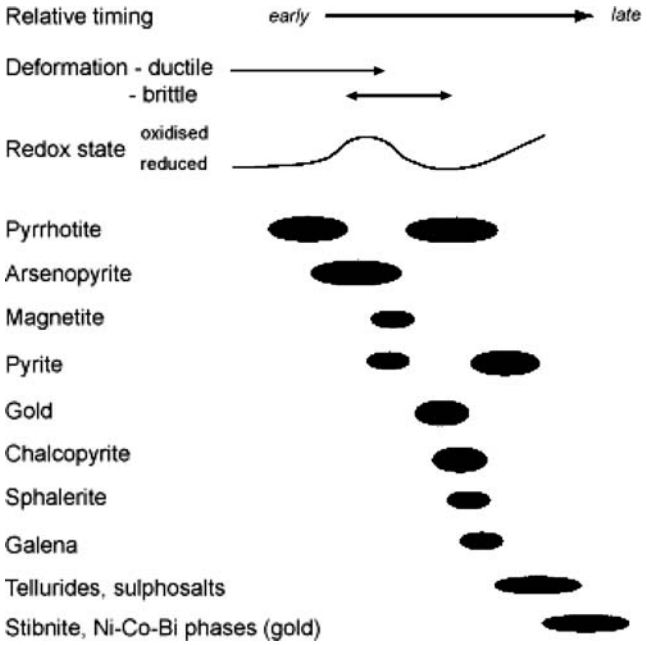

Fig. 9 Ore paragenetic sequence in the Golden Pride gold deposit based on petrographic and SEM studies

inclusions most likely represent high-pressure gas-rich (possibly CO_2 and/or CH_4) inclusions.

A correlation between arsenopyrite and gold can be observed in samples from the ore zone, but visible gold consistently post-dates the deposition of arsenopyrite. Likewise, abundant acicular to euhedral arsenopyrite occurs outside the ore zone, which is generally gold-barren.

Arsenopyrite shows subtle to quite pronounced zonation patterns when examined by SEM. In orogenic gold deposits elsewhere (e.g. Fosterville, Victoria; Bierlein et al. 2000; Bardoc Tectonic Zone, Western Australia; Morey et al. 2008), it has been shown that similar chemical zonation patterns are related to alteration of the arsenopyrite, with concurrent enrichment in gold and other elements towards the rim zones. However, EDS analysis of a number of arsenopyrite grains in the Golden Pride gold deposit has shown that the zonation is more likely to be related to deficiencies in As and substitution by Fe, rather than gold enrichment (Table 2, Electronic Supplementary Material).

Sulphur isotope study

Sulphur isotope data for a total of 29 conventional and in situ laser ablation analyses are summarised in Table 3 (Electronic Supplementary Material), with all plotted on a $\delta^{34}S$ distribution graph in Fig. 11. The $\delta^{34}S$ values for arsenopyrite (both laser ablation and conventional) range from 1.8 to 6.1 per mil. The results from analysis from pyrrhotite exhibit a wide range of $\delta^{34}S$ values. Laser ablation values for seven pyrrhotite samples range from −1.9 to 3.5 per mil, with ten conventional analyses covering an even wider spread from −5.8 to 2.6 per mil. When one considers the specific association of pyrrhotite, most of the pyrrhotite samples that display positive $\delta^{34}S$ values relate to syn-gold pyrrhotite (po_2), whereas those with lighter (i.e. negative) $\delta^{34}S$ values relate to pre-gold pyrrhotite (po_1; Fig. 11). The analysis by laser ablation of a core of a large disseminated pyrite associated with gold mineralisation yielded −1.6 per mil, whereas the rim of the same crystal gave 2.6 per mil. Pyrite from within a late-stage vein has a very light $\delta^{34}S$ value of −12.4 per mil, and the analysis of a massive pyrite vein in sandstone also yields a relatively light value of −3.3.

Discussion

The Golden Pride gold deposit—a typical Archaean orogenic gold deposit?

Based on geological characteristics, which include (1) strongly deformed host rocks, (2) overall low sulphide volume, (3) abundant quartz–carbonate veining, (4) a carbonate–sulphide–chlorite–sericite alteration assemblage in greenschist facies rocks and (5) a spatial association with large-scale compressional structures, the Golden Pride gold deposit can be classified as an orogenic gold deposit (Groves et al. 1998). On the other hand, the complex ore paragenesis, as well as the relatively high silver content of gold, is atypical of Archaean orogenic gold deposits and might point to the influence of a reduced magmatic–hydrothermal system, although the presence of tellurides and accessory Ni–Co phases do not necessarily provide support for such an influence (Hagemann and Cassidy 2000). Nevertheless, the range of $\delta^{34}S$ compositions of gold-bearing sulphides in the Golden Pride gold deposit is similar to $\delta^{34}S$ compositions from other Archaean orogenic gold deposits within, for example, the Eastern Goldfields Province of the Yilgarn Craton and elsewhere (e.g. Lambert et al. 1984; McCuaig and Kerrich 1998).

Nature of ore fluids

The overall dominance of pyrrhotite as a stable sulphide assemblage during mineralisation at the Golden Pride gold deposit, as well as the predominance of pyrrhotite over pyrite, suggests that depositional conditions were reducing and moderately acidic. This assumption is also based on the common association of pyrrhotite with muscovite and sericite in the ore zones and the incipient destruction of early magnetite and arsenopyrite during the gold-forming stage. Although post-mineralisation deformation has somewhat obscured the evidence, mineralisation appears to have

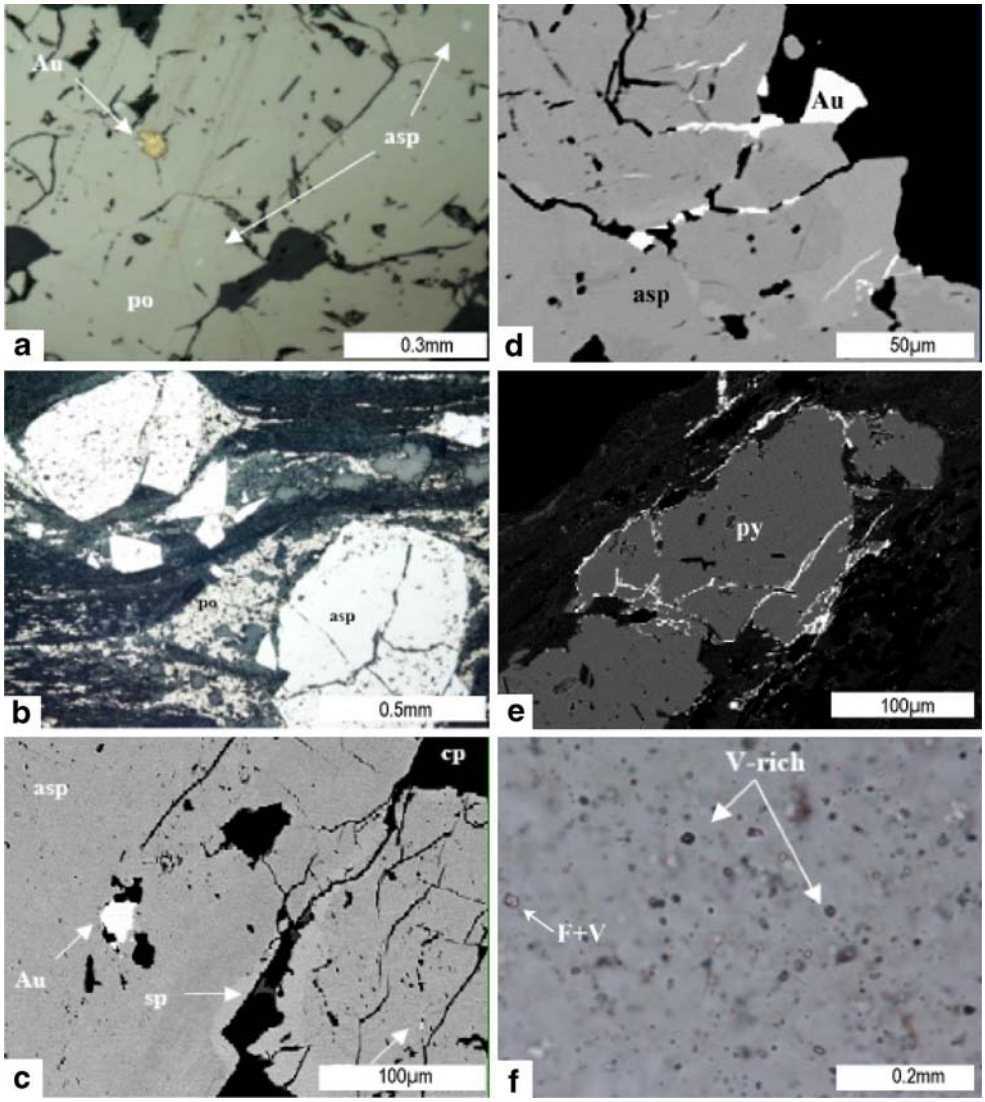

Fig. 10 **a** GPR867/190.7 m: gold (*Au*) in interstitial space at triple junction of annealed pyrrhotite (*po*), which also contains small euhedral arsenopyrite (*asp*) grains. Reflected light, plane polars. **b** GPR448/109.1 m rotated and fractured arsenopyrite (*asp*) porphyroblast, with pyrrhotite developed along cleavage planes and in pressure shadows. Visible gold (not in this image) as well as small blebs of galena and sphalerite occur within dilational fractures in the arsenopyrite. Reflected light, plane polars. **c** GPR448/109.1 m: gold (*Au*) as inclusion in subtly zoned arsenopyrite (*asp*), intergrown with chalcopyrite (*cp*), sphalerite (*sp*) and galena (*ga*). Backscattered SEM image. **d** GPR923/364.5 m: gold (*Au*) intergrown with and penetrating weakly zones arsenopyrite (*asp*). Backscattered SEM image. **e** GPR404/120.3 m: Bi–Sb–Au–S solid solution penetrating pyrite (*py*). Backscattered SEM image. **f** GPR135/235 m: abundant fluid inclusions in vein quartz. Two generations of liquid + vapour inclusions can be differentiated, whereby fluid > gas inclusions (*FL+V* on image) are dominant. Less common high-pressure gas-rich inclusions (most likely CH_4 and/or CO_2) are evidenced by the large bubbles that almost completely fill the negative crystal-shaped inclusions (V-rich on image). Transmitted light, plane polars

been controlled by a combination of (1) sulphidation of the host rocks, based on the abundance of disseminated sulphides within and around the ore zones, (2) pressure gradients, based on the presence of gold within dilational sites at all scales, and (3) subtle variations in Eh–pH conditions of the mineralising fluid, as evidenced by variations in redox and sulphur activity which affected the paragenetic sequence. Cooling of the evolving hydrothermal system during exhumation and the increase in oxidation state may have resulted in the precipitation of minor, spongy pyrite and degradation of pyrrhotite towards the final (epizonal) stage of Bi–Sb ± Au mineralisation. The presence of cobalt, nickel, tungsten and tellurium in the observed sulphide phases (Table 2, Electronic Supplementary Material), together with (rare) hyper-saline fluid inclusions and evidence of methane and/or carbon dioxide in the system (Fig. 10f), might indicate a reduced magmatic–hydrothermal contribution to gold formation.

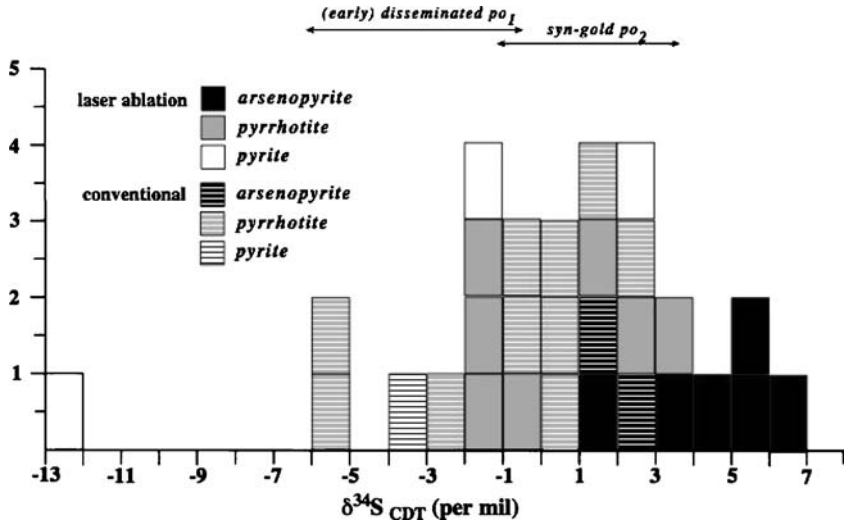

Fig. 11 Distribution of $\delta^{34}S$ (in ‰) values of iron sulphide phases from the Golden Pride gold deposit. See Table 3 (Electronic Supplementary Material) for data

Breakdown and leaching of mafic intrusions deeper in the system, which have elevated Ni and Co values (Table 1, Electronic Supplementary Material), may have supplied excess Co and Ni (and potentially Au) and contributed to the deposition of Ni and Co sulphides. Potentially, this process may have played a role in influencing mineralising fluid composition and/or redox conditions that allowed the deposition of gold.

Many world-class (i.e. ≥30 t Au) mafic-hosted gold deposits (e.g. Kalgoorlie and Kambalda gold camps, Sunrise Dam, Tarmoola, Kanowna Belle; Weinberg et al. 2002) are characterised by a relatively broad range of $\delta^{34}S$ pyrite compositions from −10 to 10 per mil. These ranges are a feature of sulphide deposition in relatively oxidised hydrothermal environments during gold mineralisation, or the occurrence of significant variations in redox conditions due to the influence of mineralising fluids from oxidised granites. Mixing between these fluids is another viable scenario to explain the variation in sulphur isotope composition. By contrast, the abundance and dominance of pyrrhotite at the Golden Pride gold deposit is evidence that overall reduced hydrothermal conditions prevailed during gold mineralisation. This is in agreement with results from sulphur isotope analyses of syn-gold po_2. The significantly lighter $\delta^{34}S$ values obtained from pyrite, particularly within a late-stage vein (Table 3, Electronic Supplementary Material), can be explained in terms of the fractionation processes under increasingly oxidised conditions (e.g. due to the consumption of H_2S during sulphide precipitation and Raleigh fractionation effects) and possibly minor contamination with sulphur from other sources.

The 'switch' from pre-ore pyrrhotite (po_1) to pyrite and back to pyrrhotite (po_2) deposition (Fig. 11) associated with gold mineralisation as indicated in the paragenetic sequence (Fig. 8), as well as measured variations in $\delta^{34}S$ values observed between the core and rim of pyrite, likely reflects changes in fO_2 and pH during fluid evolution. A minor redox change during rapid precipitation (which would have buffered the sulphur against fO_2) as implicated by the ore paragenesis could be inferred as the main cause of gold mineralisation at the Golden Pride gold deposit.

Sulphur isotope values of arsenopyrite (Table 3, Electronic Supplementary Material) suggest that the hydrothermal fluids causing arsenopyrite deposition may have been derived from metamorphism of (volcano-) sedimentary rocks that were influenced by changing fO_2 conditions (attributing to the negative values). The shift from negative $\delta^{34}S$ in po_1 to positive $\delta^{34}S$ values in po_2 implies that fluids contributing to the deposition of po_2 may have been derived from a distinct external source rather than re-mobilisation of po_1 and therefore indicate mixing of at least two sources of sulphur. Potential candidates for this source include buried (volcano-) sedimentary rocks or a homogeneous magmatic source (Ohmoto 1986). The ultimate source of the sulphur contributing to mineralisation at the Golden Pride gold deposit remains unconstrained, with the range of $\delta^{34}S$ compositions allowing for variable contributions from a volcaniclastic or magmatic source, or the metamorphic re-mobilisation of a magmatic source, and/or derivation of sulphur from more proximal local reservoirs. However, the source cannot be entirely magmatic or sedimentary, and the sulphur of syn-gold (po_2) pyrrhotite was at least in part derived from a source different to that of pre-ore (po_1) pyrrhotite.

Timing of and controls on gold mineralisation

The co-temporal and co-spatial relationship between dacitic and lamprophyric dykes and the GPSZ and related gold mineralisation suggests that a period of major tectonism and magmatism and associated gold mineralisation occurred around 2,680 Ma that formed the Golden Pride gold

deposit. In particular, the presence of lamprophyric dykes is a common feature of many orogenic gold deposits (e.g. Kerrich and Wyman 1994; Borg and Krogh 1999). Kerrich and Wyman (1994) indicated that the co-temporal and co-spatial relationship between lamprophyres and gold mineralisation in a number of deposits in the Superior Province of Canada may suggest that both have been emplaced along trans-lithospheric structures that demark sub-province boundaries. These authors considered that a transpressional tectonic regime and in particular uplift and decompression following oblique collision of allochthonous terranes could explain the coincidence of gold and lamprophyres in these deposits. Similar implications can be made for the Golden Pride gold deposit, where both reverse and sinistral movement has been observed along the GPSZ. This would suggest that the GPSZ is a regionally important potentially trans-lithospheric structure that represents a suture that accommodated amalgamation of allochthonous terranes. Moreover, the GPSZ provided a pathway for the emplacement of a variety of intrusions that may have further contributed to local injection of mineralising fluids. Overall, analyses of mafic intrusions (lamprophyric dykes) at Golden Pride indicate the absence of gold in these intrusions. However, some of the mafic intrusions indicate low levels of gold mineralisation (Table 1, Electronic Supplementary Material), and their W–As–Au signature suggests that they may be affected by a hydrothermal overprint. The presence of both unmineralised and mineralised (hydrothermally altered) mafic intrusions at Golden Pride further corroborates that the emplacement of these dykes and the circulation of gold-bearing fluids overlap in time.

It is inferred that the GPSZ has a long-term history of ductile deformation and repeated re-activation. On a macro-scale, opposing kinematic indicators and transposition of early fabrics support this notion. On a micro-scale, textural relationships such as the rotation and fracturing of sulphides and the presence of pressure shadows, with a semi-penetrative cleavage wrapped around arsenopyrite porphyroblasts (Fig. 10e), also support this notion. The latter observations suggest that ductile deformation associated with movement along the GPSZ already occurred prior to gold deposition and affected the initial post-peak metamorphic assemblage resulting in solid solution re-mobilisation of early sulphides (pyrrhotite, arsenopyrite).

In terms of a genetic model explaining the occurrence of the Golden Pride gold deposit along a regional shear zone, it is considered that following regional deformation (accretion), the GPSZ formed a ‘backbone’ (see Cox 1999) that allowed hydrothermal fluids to pass through the crust. The presence of sericite–chlorite-altered greenschist facies sedimentary host rock suggests that mineralisation occurred in reduced, acidic environments at temperatures around 300°C. In the area of the Golden Pride deposit, a coincidence of a number of factors is considered to have generated a favourable site for ore deposition. These include: 1) *Structural setting*. The presence of WSW-ENE trending cross-structures that interacted with intensely deformed sandstone-siltstone packages in the hanging-wall (i.e. discharge part of the system) of the GPSZ, and subsidiary structures like the HWS and other fault elements, which would have promoted fluid focussing. In addition, inflections along the GPSZ (Fig. 7) may have allowed further fluid focussing and gold deposition, in particular along sandstone units that are considered to have a higher porosity then surrounding siltstone units; 2) *Chemical setting*. A redox contrast related to the interaction of oxidising fluids (possibly emanating from mafic intrusions with lamprophyric affinity) with reducing fluids circulating in the sedimentary rock package. Mixing of these fluids may have affected gold solubility and could have controlled the precipitation of gold from gold-bearing fluids (Cox et al. 1995).

Summary and exploration significance

As revealed by detailed surface and drill core studies, the Golden Pride gold deposit is hosted in a dominantly metasedimentary rock package that has been intruded by mafic dykes with lamprophyric affinities, as well as intermediate to felsic dykes. The rock package is intensely deformed in the immediate hanging wall of the GPSZ, which has acted as a (regional) conduit for hydrothermal fluids. Petrographic and geochemical studies indicate that mineralising fluids have been directed towards dilational sites (on all scales), with gold deposition in response to subtle changes in redox conditions in an overall reducing environment. A paragenetic change from pre-gold pyrrhotite–arsenopyrite assemblages to syn-gold pyrrhotite–pyrite ± chalcopyrite assemblages with distinct $\delta^{34}S$ characteristics attests to the influence of at least two sources of sulphur in the mineralising fluids.

The presence of several intrusions of different chemistry/timing in dilational sites (e.g. jogs and bends) along the GPSZ can be used as a targeting tool for gold within the Nzega Greenstone Belt. Most likely, the location of the Golden Pride gold deposit in the hanging wall of a regionally important potentially trans-lithospheric shear zone, together with the occurrence of a variety of intrusions (which are not observed elsewhere along the GPSZ), may have been controlled by the intersection of the GPSZ with inferred WSW–ENE trending structure(s). The recognition of this important structural control should be built into regional targeting models for gold in the Nzega Greenstone Belt and elsewhere in the Lake Victoria Goldfields. The findings reported herein, when combined with additional

studies on gold deposits elsewhere in the Archaean Craton of Tanzania, will contribute to the development of a regionally consistent and comprehensive synthesis on the tectonic evolution of the LVG. This, in turn, will assist in the development of tectono-metallogenic models for gold deposition in the Archaean Craton of Tanzania.

Acknowledgements The authors wish to express their gratitude to Jigsaw Geoscience Pty. Ltd.'s Kas De Luca and Ian Neilson for their valuable contributions. In addition, Scott Halley of Mineral Mapping Pty. Ltd. has contributed his geological knowledge, in particular in relation to lithogeochemistry and recognising the various alteration styles. Prof. Anthony J. Crawford (University of Tasmania) and Dr. Doug Mason (Mason Geoscience Pty. Ltd.) both conducted petrographical studies, respectively, on intrusive and sedimentary (as well as ore-related) rocks from the Golden Pride gold deposit that contributed to the understanding of the lithologies and mineralisation styles. Stafford McKnight has dedicated his time and knowledge to assist with SEM work at the University of Ballarat. Andrew Goode is thanked for reviewing an early version of the manuscript and providing valuable comments. The authors wish to acknowledge the support of the CEO and General Manager Exploration from Resolute Mining Ltd. in approving publication of this paper. Revision of the manuscript was aided by constructive comments from the reviewers Basem Zoheir and Gregor Borg, and the editor, Bernd Lehmann. Their support is greatly appreciated.

References

Bierlein FP, Arne DC, McKnight S, Lu J, Reeves S, Besanko J, Marek J, Cooke D (2000) Wall-Rock petrology and geochemistry in alteration halos associated with mesothermal gold mineralisation, Central Victoria, Australia. Econ Geol 85:283–311

Borg G (1990) A preliminary report on the geology of the Siga Hills, NW Tanzania. Part I: Regional geology, geophysics, geochemistry and distribution of gold within the project area: Tanzanian–German Technical Cooperation, BGR internal report, Archive no. 108564. pp77.

Borg G, Krogh T (1999) Isotopic age data of single zircons from the Archaean Sukumaland Greenstone Belt, Tanzania. J Afr Earth Sci 29:301–312

Borg G, Shackleton RM (1997) The Tanzania and NE Zaire cratons. In: DeWit M, Ashwal LD (eds) Greenstone belts. Oxford University Press, Oxford, pp 608–619

Chamberlain CM, Tosdal RM (2007) U–Pb geochronology of the Lake Victoria Greenstone Terranes. Confidential report to project sponsors. Mineral Deposits Research Unit, University of British Columbia, Vancouver, BC 81p

Cox SF (1999) Deformational controls on the dynamics of fluid flow in mesothermal gold systems. Geol Soc Lond Spec Pub 155:123–140

Cox SF, Sun SS, Etheridge MA, Wall VJ, Potter TF (1995) Structural and geochemical controls on the development of turbidite-hosted gold–quartz vein deposits, Wattle Gully Mine, central Victoria, Australia. Econ Geol 90:1722–1746

Groves DI, Goldfarb RJ, Gebre-Mariam M, Hagemann SG, Robert F (1998) Orogenic gold deposits: a proposed classification in the context of their crustal distribution and relationship to other gold deposit types. Ore Geol Rev 13:7–27

Groves DI, Goldfarb RJ, Robert F, Hart CJR (2003) Gold deposits in metamorphic belts: overview of current understanding, outstanding problems, future research and exploration significance. Econ Geol 98:1–19

Hagemann SG, Cassidy KF (2000) Archaean orogenic lode gold deposits. Rev Econ Geol 13:9–68

Harpum JR (1970) Summary of the geology of Tanganyika. Part V; structure and geotectonics of the Precambrian. Geol Surv Tanganyika Mem 2:1–58

Huston DL, Power M, Gemmell JB, Large RR (1995) Design, calibration and geological application of the first operational Australian laser ablation sulphur isotope microprobe. Aust J Earth Sci 42:549–555

Kabete JM, Groves DI, McNaughton NJ, Mruma AH (2008) A new tectonic subdivision of the Archean of Tanzania and its significance to gold metallogeny. SEG-GSSA 2008 Africa Uncovered Conference—Abstr Vol, pp 21–25

Kerrich R, Wyman DA (1994) The mesothermal gold-lamprophyre association: significance for an accretionary geodynamic setting, supercontinent cycles, and metallogenic processes. Mineral Petrol 51:147–172

Lambert IB, Phillips GN, Groves D (1984) Sulphur isotope compositions and genesis of Archaean gold mineralisation, Australia and Zimbabwe. In: Foster RP (ed) Gold '82; the geology, geochemistry and genesis of gold deposits, Geol Soc Zimbabwe. Balkema, Rotterdam, pp 373–387

McCuaig TC, Kerrich R (1998) P-T-t-deformation-fluid characteristics of lode-gold deposits: evidence from alteration systematics. Ore Geol Rev 12:381–453

Morey AA, Tomkins AG, Bierlein FP, Weinberg RF, Davidson GJ (2008) Bimodal distribution of gold in pyrite and arsenopyrite: examples from the Archaean Boorara and Bardoc Shear Systems, Yilgarn Craton, Western Australia. Econ Geol 103:599–614

Ohmoto H (1986) Stable isotope geochemistry of ore deposits. In: Valley JW, Taylor HP, O'Neil JR (eds) Stable isotopes in high temperature geological processes. Reviews in Mineralogy 16. Mineralogical Society of America, Washington, DC, pp 491–560

Stevens R, Kennedy R (1998) The Golden pride Gold Deposit Tanzania. AIG Bull 25:3–8

Tulloch AJ, Kimbrough DL (2003) Paired plutonic belts in convergent margins and the development of high Sr/Y magmatism: Peninsular Ranges batholith of Baja-California and Median Batholith of New Zealand. Geol Soc Am Spec Publ 374:275–295

Vos IMA, Halley SH, Christie MHD (2007) Targeting Gold deposits along a regional shear zone: a case study from the Archaean Golden Pride deposit in Tanzania. In: Milkereit B (ed) Proceedings of Exploration 07: Fifth Decennial International Conference on Mineral Exploration, pp 953–956

Weinberg RF, Groves DI, Hodkiewicz PF, Van Der Borgh P (2002) Hydrothermal systems, giant ore deposits and a new paradigm for predictive mineral exploration. AMIRA Project P511, Yilgarn Atlas Vol. 3 (unpubl.), pp 140–170

Wilson M (1989) Igneous petrogenesis. Kluwer, Dordrecht p 450